PHYSICAL REVIEW B VOLUME 27, NUMBER 4 15 FEBRUARY 1983

Two-photon spectroscopy of B excitons in CdS

D. G. Seiler
Center for Applied Quantum Electronics, Department of Physics, North Texas State University, Denton, Texas 76203

D. Heiman
Francis Bitter National Magnet Laboratory, Massachusetts Institute of Technology, Cambridge, Massachusetts 02139

B. S. Wherrett
Department of Physics, Heriot-Watt University, Edinburgh, Scotland
(Received 13 October 1982)

High-resolution spectra are obtained for the free A and B excitons in CdS by two-photon absorption photoconductivity techniques at 1.8 K. At zero applied magnetic field, spectra are shown which indicate for the first time the presence of anisotropy splitting of the $B(2P)$ exciton states. The first observation of the $B(3P)$ exciton state at $B=0$ T then allows the conclusion that both the effective Rydberg and the anisotropy parameter of the A and B excitons are the same. This further indicates that the A and B valence-band masses are equal. These conclusions are confirmed by the first observation of the Zeeman splitting of the $B(2P_{\pm 1})$ and $B(3P_{\pm 1})$ exciton states at fields up to 10 T. Fine-structure splitting of the $B(2P_{+1})$ and $B(2P_{-1})$ states results from an effective g factor for the B valence band of $g_h^B=0.7\pm 0.3$.

INTRODUCTION AND BACKGROUND

There have been a number of studies over the past 20 years that have provided detailed information about the nature of the free A exciton in CdS and its behavior in a magnetic field. Linear spectroscopy using one-photon absorption, one-photon emission or luminescence, or one-photon reflectance techniques allowed various features of the magneto-optical effects in the A-exciton spectrum to be investigated.[1-7] The primary features were Zeeman splittings and diamagnetic shifts from which effective masses and g factors for the conduction band and A valence band were extracted. The A-exciton spectra of cadmium sulfide has also been extensively investigated using two-photon absorption (TPA) techniques.[8-14] This form of nonlinear spectroscopy has several advantages over one-photon spectroscopy: (1) less sensitivity to crystal surface quality and crystal thickness (since TPA is a bulk effect); (2) different selection rules allowing different eigenstates to be investigated; and (3) more transitions are possible because of the flexibility of using two photons of different polarization.

The A valence band as well as the conduction band have been well characterized in previous studies (see Table IV of Ref. 14). In contrast, little information is available about the B valence band. This is due to the difficulty in obtaining well-resolved free-exciton spectra. In this paper we investigate free excitons associated with the B valence band using two-photon spectroscopy techniques. Application of a magnetic field allows Zeeman splittings and diamagnetic shifts of the B—free-exciton states to be observed. The results and analysis provide new, quantitative information about the B valence band.

High-purity, single-crystal platelets of CdS were used in the as-grown condition. "Good" crystals [those showing clear resolution of the $A(2P_0)$ lines at $B=0$ with full width at half maximum (FWHM) linewidths ~ 0.3 meV] had dark-room-temperature resistivities $>10^6$ Ω cm. The free-exciton spectra were taken by observing the increase in light absorption as monitored by the increase in sample conductivity as a function of photon energy. This has previously been shown to be a sensitive method of investigating TPA effects in InSb (Refs. 15 and 16) with cw lasers and in CdS (Ref. 14) with pulsed lasers.

A Q-switched yttrium aluminum garnet laser was used to produce two light beams, one tunable ($1700<\hbar\omega_v<1834$ meV) from a dye laser and the other fixed at $\hbar\omega_{ir}=784$ meV produced by stimulated Raman scattering.[17] The visible and infrared (ir) beams were made to overlap in time and were com-

bined collinearly before being focused onto the sample. The samples were mounted in a Dewar containing pumped liquid He at 1.8 K. The optical Dewar tail was mounted in a 2-in. Bitter magnet solenoid having radial access to the light in a Voigt configuration. The applied current, c axis, and B field were all parallel. Spectral scans were taken via a computer that read the photoinduced voltage from a boxcar integrator with an analog-to-digital converter while scanning the tunable dye laser through a stepping-motor-shaft-encoder combination.

From the group theory of the C_{6v} double group one can determine both the radiation selection rules for the excitonic states of CdS and the nature of the magnetic field splittings of the various levels. A full analysis for the A-exciton problem was summarized by Seiler *et al.*[14] for Γ-point transitions. Specific results pertaining to one-photon absorption of the B *excitons* are given by Mahan and Hopfield[18] and for two-photon absorption (in ZnO) by Dinges *et al.*[19] The symmetries of the B exciton at the Γ point, are obtained from the direct product of the Γ_7 conduction-band symmetry, the Γ_7 (B) valence-band symmetry, and the symmetry of the hydrogenic functions (Γ_1 for S or P_0 functions, Γ_5 for the pair of $P_\pm$ functions).

Radiation selection rules for both one- and two-photon absorption follow from this while recognizing that the radiation-matter interaction has symmetry Γ_1 for the electric field parallel to the crystal c axis ($\vec{E}||c$) and Γ_5 for $\vec{E}\perp c$. Two-photon interactions thus have the symmetries Γ_1, Γ_5 and $(\Gamma_1+\Gamma_2+\Gamma_6)$, respectively, for the configurations $(||,||)$, $(||,\perp)$, and $(\perp,\perp)$. The allowed radiative transitions ($\Gamma_{\text{exciton}}\times\Gamma_{\text{interactions}}$ containing the symmetric irreducible representation) are summarized in Table I, for the zero magnetic field case.

To obtain expressions for the magnetic field splittings of either transitions requires the forms of the exciton eigenfunctions. The presence of splitting can alternatively be deduced from consideration of the symmetry of the field itself, either as a perturbation in the C_{6v} symmetry group, or as the cause of symmetry reduction to C_6. For all but the $2\Gamma_5(P_{\pm1})$ states, the eigenfunctions are easy to find. They are just the symmetry adapted basis functions based upon the Γ_7 conduction, Γ_7 valence, and hydrogenic functions. The valence-band eigenfunctions are discussed by Mahan and Hopfield.[18] Ignoring the $\vec{k}\cdot\vec{p}$ mixing of the bands, and omitting the relatively small spin-orbit mixing of the Z states into the B levels the essential form of the eigenfunctions is given by $(X+iY)\downarrow_h$ and $(X-iY)\uparrow_h$. The conduction states we term $\uparrow_e$ and $\downarrow_e$. Symmetry adapted exciton functions are included in Table I. The Γ_5 pair are degenerate in the absence of an applied magnetic field. The Γ_1,Γ_2 states are, strictly speaking, the antisymmetric and symmetric combinations of the functions shown. When the field splitting is larger than the crystal-field splitting of the excitonic levels, then the eigenfunctions will be those Γ_1,Γ_2 combinations of specific spins (the functions written out). Only the $2\Gamma_5(P_{\pm1})$ states are not uniquely specified by group-theoretical analysis; they are appropriate linear combinations of the four functions shown. We will not consider this case any further since the $(||,\perp)$ geometry was not used in the present experiment.

For states other than $\Gamma_5(P_{\pm1})$ we obtain the magnitude of the g value by defining the conduction-band spin-splitting, $\uparrow_e-\downarrow_e$, to be $g_e\mu_B B$, the valence splitting,

$$(X+iY)\downarrow_h-(X-iY)\uparrow_h ,$$

TABLE I. CdS B-exciton states and their symmetries. The allowed one- and two-photon transitions and their polarizations are shown for $\vec{E}\perp\vec{c}$ and $\vec{E}||\vec{c}$. The corresponding eigenfunctions and g values in the presence of a magnetic field $\vec{B}||\vec{c}$ are also given.

State	Symmetries	Polarization: One-photon	Polarization: Two-photon	Eigenfunctions	g values
S,P_0	Γ_5	$\perp$	$(||,\perp)$	$(X+iY)\downarrow_h\uparrow_e S,P_0$ $(X-iY)\uparrow_h\downarrow_e S,P_0$	$\lvert g_h^B+g_e\rvert$
	Γ_2		$(\perp,\perp)$	$(X+iY)\downarrow_h\downarrow_e S,P_0$	$\lvert g_h^B+g_e\rvert$
	Γ_1	$\|\|$	$(||,||)$ or $(\perp,\perp)$	$(X-iY)\uparrow_h\uparrow_e S,P_0$	
$P_\pm$	Γ_6		$(\perp,\perp)$	$(X+iY)\downarrow_h\uparrow_e P_+$ $(X-iY)\uparrow_h\downarrow_e P_-$	$\lvert 2g_\mu^B+g_h^B+g_e\rvert$
	$2\Gamma_5$	$\perp$	$(||,\perp)$	$(X+iY)\downarrow_h\downarrow_e P_\pm$ $(X-iY)\uparrow_h\uparrow_e P_\pm$	
	Γ_2		$(\perp,\perp)$	$(X+iY)\downarrow_h\uparrow_e P_-$	$\lvert 2g_\mu^B-g_h^B-g_e\rvert$
	Γ_1	$\|\|$	$(||,||)$ or $(\perp,\perp)$	$(X-iY)\uparrow_h\downarrow_e P_+$	

to be given by g_h^B and the hydrogenic orbital splitting, $P_+ - P_-$, by $2g_\mu^B$. The tabulated g values follow from the forms of the eigenfunctions. A further consequence of the field is that the selection rules for the Γ_1, Γ_2 states become mixed; thus, for both states one-photon absorption is allowed for $\vec{E}||c$ and two-photon absorption for either $(||,||)$ or $(\perp,\perp)$ configurations.

RESULTS

B=0

TPA results for the free B excitons at zero magnetic field are shown in Fig. 1 in the upper three traces. Also shown for direct comparison is a high-resolution TPA spectra for the A excitons. Several conclusions can be drawn from this figure. (1) The quality of these CdS crystals is "good" because there is a clear resolution of the splitting between the

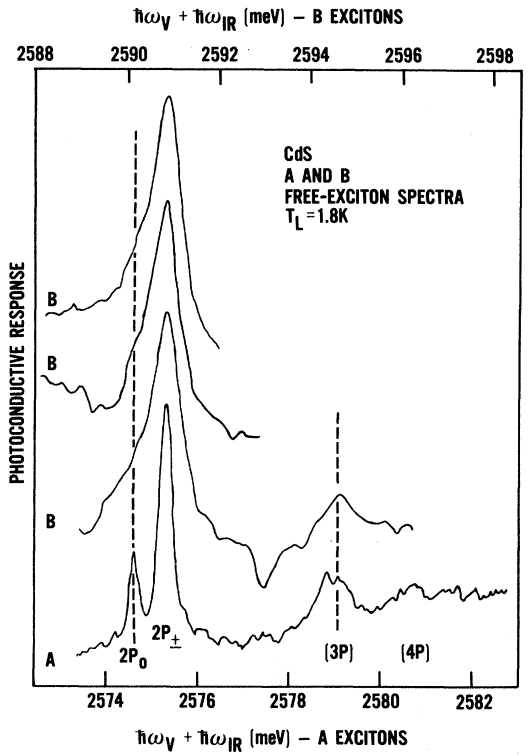

FIG. 1. Two-photon photoconductivity spectra for the A and B free excitons in CdS at $B=0$ T. The bottom trace A shows the high resolution of the A excitons with the $A(2P_0)-A(2P_{\pm1})$ anisotropy splitting clearly resolved. The three upper traces show spectra of the B excitons which have a much larger linewidth. The presence of a $B(2P_0)$ component is indicated by the asymmetric lineshape in the vicinity of the dashed line near the $2P_0$ state. The instrumental resolution of 0.1 meV is narrower than the intrinsic linewidth of the excitons.

$A(2P_0)$ and $A(2P_{\pm1})$ spectral positions. The FWHM linewidth for the $A(2P_{\pm1})$ state is 0.3 meV. The signal-to-noise ratio is also sufficient to resolve the $n=3$ and $n=4$ A excitons at $B=0$ T. A more detailed analysis of these $A(2P)$ and $A(3P)$ excitons was presented earlier by Seiler *et al.*[14] Clearly, the B excitons have a much larger FWHM linewidth (values from $\sim 0.7 \rightarrow 1.1$ meV have been observed in "good" crystals, with an average over five spectral runs equal to ~ 0.9 meV). The B-exciton lines are broader because their lifetimes are shorter than those of the A excitons. (2) Since the B excitons have larger linewidths, it has been difficult to observe the anisotropy splitting between the $B(2P_0)$ and $B(2P_{\pm1})$ states. However, we show in Fig. 1 three spectral scans of the $B(2P)$ region that consistently show strong evidence for the presence of the $B(2P_0)$ component as indicated by the asymmetry in the line shape. Although the $B(2P_0)$ state is not clearly resolved, we estimate that its position is at 2590.2 ± 0.2 meV. In spectra where a good baseline could be established, subtracting off a large symmetric $B(2P_{\pm1})$ peak, resulted in a peak at this position. This is *the first* observation of this state. The anisotropy splitting of the $B(2P)$ state is thus estimated to be

$$B(2P_{\pm1})-B(2P_0)=0.6\pm0.2 \text{ meV},$$

compared to that of the $A(2P)$,

$$A(2P_{\pm1})-A(2P_0)=0.69\pm0.02 \text{ meV}.$$

(3) The energy separations between the $3P_{\pm1}$ and $2P_{\pm1}$ states are also the same within the uncertainties. For the A exciton, this splitting is 3.97 ± 0.11 meV and for the B exciton 3.8 ± 0.2 meV. This also represents the *first time* that the $B(3P)$-exciton state has been observed. See also Fig. 2 at $B=0$ for a clear resolution of the $B(3P)$-exciton state.

Several important conclusions can now be made from these observations. Points (2) and (3) give strong support that the effective Rydberg R_y^* $(=\mu_\perp e^4/2\hbar^2K^2)$ and the anisotropy parameter γ $(=\mu_\perp K_\perp/\mu_{||}K_{||})$ of the B excitons are equal to those of the A excitons. Thus

$$R_y^{*B}=R_y^{*A}=27.4\pm0.8 \text{ meV}$$

and

$$\gamma^B=\gamma^A=0.797\pm0.013$$

(see Ref. 14 for the A-exciton values). Assuming $K_\perp$ and $K_{||}$ are the same for both the A- and B-exciton regions implies that

(i) $\mu_\perp^B=\mu_\perp^A=(0.158\pm0.002)m_0$

and

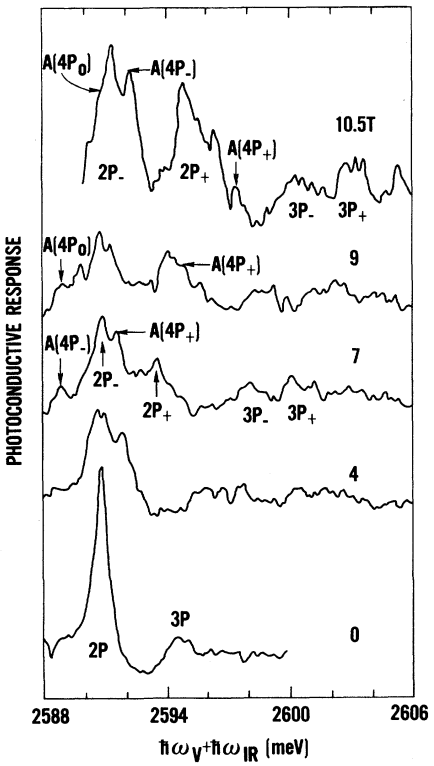

FIG. 2. Photoconductive response vs total photon energy $\hbar\omega_v + \hbar\omega_{ir}$ near the B-exciton region for various magnetic fields. The magnetic field $\vec{B}$ was parallel to the hexagonal c axis in a Voigt configuration with $\vec{E}$ perpendicular to c for the two photons at a lattice temperature of $T_L = 1.8$ K. The presence of the overlapping $A(4P)$ excitons is indicated.

$$m_{h\perp}^B = m_{h\perp}^A = (0.64 \pm 0.02) m_0$$

[using $m_e = (0.210 \pm 0.003)\ m_0$] and (ii) $\mu_{||}^B = \mu_{||}^A$ or $m_{h||}^B = m_{h||}^A$.

Table II shows the results of previously measured values of the excited B-exciton states and the results of this study. Our position for the $B(2P_{\pm 1})$ state is in excellent agreement with the TPA studies of Stafford and Sondergeld[9] and Jackel and Mahr.[13] Taking into account the anisotropy by using Faulkner's analysis as was done for the A exciton[14] determines the B energy gap to be

$$E_g^B = 2598.0 \pm 0.2 \text{ meV} .$$

Hopfield and Thomas[2] determined the position of a $B(n=2)$ state to be 2590.8 eV, which is in excellent agreement with our $B(2P_{\pm 1})$ level [presumably their state was a $B(2S)$ level because they used one-photon spectroscopy].

B≠0

The application of a magnetic field allows shifts and Zeeman splittings of individual exciton states to be measured. In fact, magneto-optical studies allow determination of exciton parameters and the corresponding energy-band parameters of the semiconductor. Figure 2 shows the effect of the magnetic field on the B—free-exciton spectra. At $B=0$ T both the $B(2P)$ and the $B(3P)$ are clearly seen. A study of Fig. 2 shows one major feature: the $B(2P)$ state splits into two parts, presumably $2P_{+1}$ and $2P_{-1}$ states. At fields >7 T, there also appears to be a fine-structure splitting to these $2P_{\pm 1}$ states. We shall return to this feature later. At fields >6 T, the $B(2P)$ spectral region becomes very complex due to the overlapping of the $A(4P_0, 4P_{\pm 1})$-exciton states. The energy positions of these photoconductive peaks are plotted in Fig. 3 as a function of magnetic field. This shows the complex nature of the exciton structure and can be used to identify the spectral features shown in Fig. 2. We also point out that this is *the first time* the magnetic field dependence of the $A(4P)$ excitons has been determined. The $B(2P_0)$ state could not be identified in any of the spectral features present at finite magnetic fields.

According to Table I for $(\perp,\perp)$ polarization two exciton states of symmetry $\Gamma_1+\Gamma_2$ and Γ_6 can be observed with effective g factors of $|2g_\mu^B - g_e - g_h^B|$

TABLE II. Measured values of excited B-exciton states (in meV).

Energy level	One-photon emission [Litton *et al.* (Ref. 4)]	Two-photon absorption Nguyen *et al.* (Ref. 10)	Stafford and Sondergeld (Ref. 9)	Jackel and Mahr (Ref. 13)	Present work
$2S$	2585.2				
$2P_0$					2590.26±0.2
$2P_{\pm 1}$		2593.5	2590.5	2590.8	2590.86±0.05
$3S$	2589.2				
$3P_0$					
$3P_{\pm 1}$					2594.6±0.1
$4S$	2590.7				

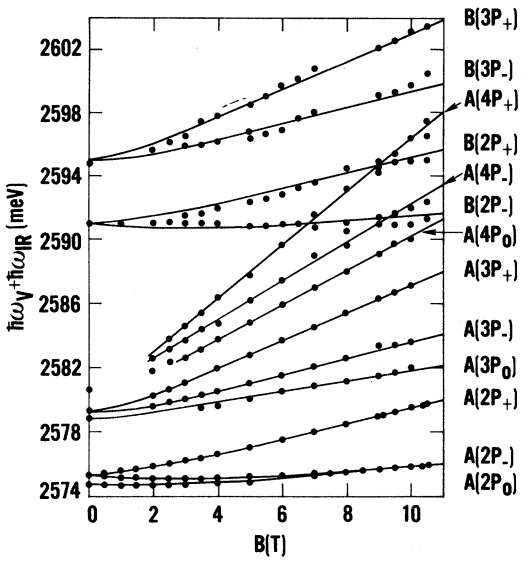

FIG. 3. Peak positions in total photon energy $\hbar\omega_v + \hbar\omega_{ir}$, for the $A(2P)$, $A(3P)$, $A(4P)$, $B(2P)$, and $B(3P)$ excitons as a function of applied magnetic field B. The solid points were determined experimentally while the lines for the $A(2P)$ and $A(3P)$ represent the variational calculations done in Ref. 14. Straight lines are drawn through the $A(4P)$ levels. The lines drawn through the $B(2P_{\pm})$ and $B(3P_{\pm})$ points are the same as the theoretical variations of the $A(2P_{\pm})$ and $A(3P_{\pm})$ levels.

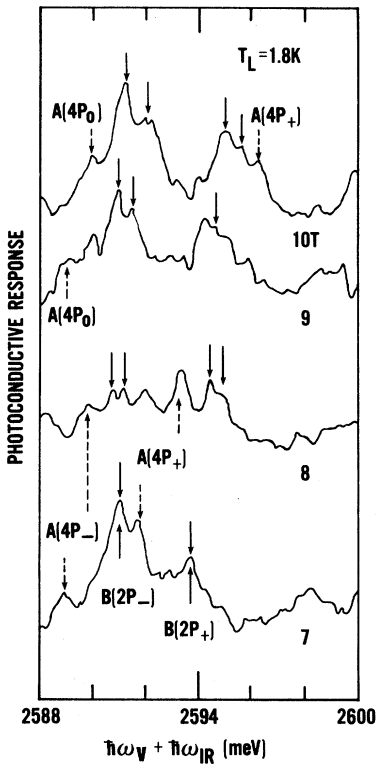

FIG. 4. High-resolution photoconductive spectral scans in the region of the $B(2P)$ exciton at various magnetic fields. The dashed lines show the overlapping $A(4P)$ excitons, while the solid arrows pointing down indicate the fine-structure splitting.

and $|2g_{\mu}^{B}+g_e+g_h^{B}|$, respectively. The Zeeman splittings are given by $\Delta E=g_{\rm eff}\mu_B B$, where μ_B is the Bohr magneton. Thus the average splitting of these two symmetry states is given by

$$|2g_{\mu}^{B}| = 6.4\pm0.4$$

from our data. Using the definition of

$$g_{\mu}^{B}=m_0(1/m_{h\perp}^{B}-1/m_{e\perp})$$

and

$$m_{e\perp}=0.210\pm0.003m_0$$

gives $m_{h\perp}^{B}=0.64\pm0.17m_0$. This mass value is the same as that of the A band which agrees with the conclusions of the zero magnetic field results discussed earlier.

The fine-structure splitting of the $B(2P_{\pm})$ states can be used to determine g_h^{B} from $g_{\rm eff}=|g_e+g_h^{B}|$. For fields ≥ 7 T, the fine-structure splitting of these states does appear to be evident in Fig. 4, indicated by the down-pointing arrows. From the experimental splitting, $g_{\rm eff}=1.1\pm0.3$, which along with $g_e=-1.78$ gives $g_h^{B}=0.7\pm0.3$. Also shown by dashed arrows are the $A(4P_0,4P_{\pm})$ exciton states. At 9 T the region around the $B(2P_{\pm})$ is rather complex making identification of the spectral features difficult. We point out that these spectral features are *reproducible from run to run.*

The high resolution obtainable by the two-photon spectroscopy technique is illustrated in Fig. 5, where a spectral scan over both the A- and B-exciton regions at $B=10$ T reveals a wealth of structure. Principal features that can be clearly identified are shown. Additional structure is present which has not been identified as yet. Again we point out that the photoconductive spectral features are reproducible, so that each peak no matter how small is physically meaningful. The dominant spectral features arise from the excitons and not just transitions between Landau levels. This conclusion is in contrast to an earlier conclusion by Shah and Damen[3] that excitonic effects are apparently not important for $N\geq 2$, where N is the Landau-level number.

The lines plotted in Fig. 3 for the $A(2P)$ and $A(3P)$ excitons represent the theoretical dependence obtained from variational calculations as explained in Ref. 14. Straight lines are drawn through the data points representing the $A(4P)$ states; no attempt was made to calculate their dependence on

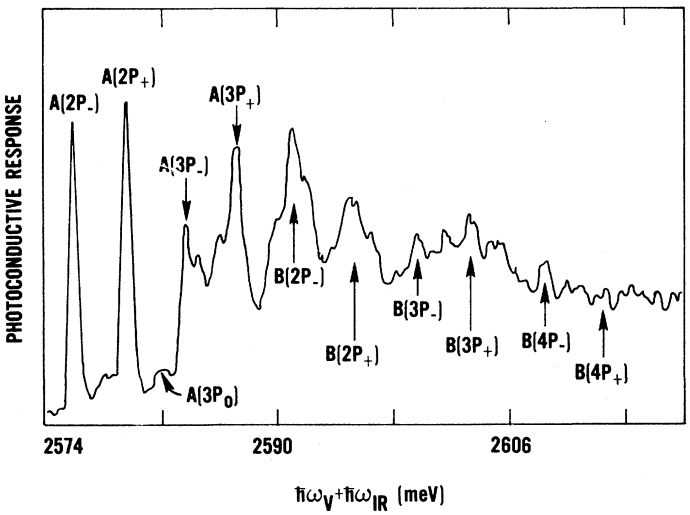

FIG. 5. High-resolution two-photon spectra for $B=10$ T, showing the complexity of the A- and B-exciton struture.

field because of the difficulty of carrying out variational calculations for the higher excited states. The lines shown for the $B(2P)$ and $B(3P)$ states are the shifted replicas of the theoretical variation of the $A(2P_{\pm1})$ and $A(3P_{\pm1})$ states with magnetic field. Consequently, the good correspondence shown in Fig. 3 reflects the fact that the parameters of the B exciton are very similar to those of the A exciton.

SUMMARY AND CONCLUSIONS

The results of our two-photon spectroscopy measurements and analysis are shown in Table III along with the few values determined by other experiments and the theoretical results of Mahan and Hopfield.[18] Our results for γ, $m_{h\perp}^B$, and g_h^B differ most significantly from the values estimated previously as shown in Table III. We believe that our measurements represent the most direct and hence most accurate means of determining these values at present.

In summary, we have for the *first time* (1) shown evidence for the anisotropy of the B valence band by giving evidence for the presence of the $B(2P_0)$ exciton at $B=0$ T, (2) observed the $B(3P)$ exciton at $B=0$ T, (3) determined the magnetic field dependence of the $A(4P_0,4P_{\pm1})$ excitons, (4) observed Zeeman splitting of the $B(2P_{\pm1})$- and $B(3P_{\pm1})$-exciton levels, and finally (5) given evidence for the fine-structure splitting of the $B(2P_{+1})$- and $B(2P_{-1})$-exciton states. Consequently, we can conclude that two-photon spectroscopy is a valuable technique of investigating semiconductor energy-band structures.

ACKNOWLEDGMENTS

We thank D. Reynolds and C. Litton for supplying the excellent quality CdS crystals and D. Spears

TABLE III. CdS B-exciton and B-band parameters.

Reference	R_y^* (meV)	γ	$\mu_\perp (m_0)$	$m_{h\perp}^B (m_0)$	E_g^B (eV)	g_h^B
This paper	27.4	0.797	0.158	0.64±0.17	2598.0±0.2	0.7±0.3
Blattner *et al.* (Ref. 7)				1.1		1.8
Koteles and Winterling (Ref. 20)				1.0±0.1		
Broser and Rosenzweig (Ref. 21)				1.1		
Mahan and Hopfield (Ref. 18)		$\sim10^{-2}$	0.17	1.0−1.2		
Segall and Marple (spherical-band approximation) (Ref. 22)			0.156		2598.1	

of Lincoln Laboratory for his help in making electrical contacts on the samples. The work of one of us (D. G. S.) was supported in part by the U. S. Office of Naval Research and experimentally carried out at the Francis Bitter National Magnet Laboratory, which is supported by the National Science Foundation.

---

[1]D. G. Thomas and J. J. Hopfield, Phys. Rev. 116, 573 (1959).

[2]J. J. Hopfield and D. G. Thomas, Phys. Rev. 122, 35 (1961).

[3]J. Shah and T. C. Damen, Solid State Commun. 9, 1285 (1971).

[4]C. W. Litton, D. C. Reynolds, and T. C. Collins, Phys. Rev. B 6, 2269 (1972).

[5]H. Venghaus, S. Suga, and K. Cho, Phys. Rev. B 16, 4419 (1977).

[6]I. Broser and M. Rosenzweig, Phys. Rev. B 22, 2000 (1980).

[7]C. Blattner, G. Kurtze, G. Schmeider, and C. Klingshirn, Phys. Rev. B 25, 7413 (1982).

[8]F. Pradere and A. Mysyrowicz, in *Proceedings of the Tenth International Conference on the Physics of Semiconductors,* edited by S. P. Keller, J. C. Hensel, and F. Stern (U. S. Atomic Energy Commission, Washington, D.C., 1970), p. 101.

[9]R. G. Stafford and M. Sondergeld, Phys. Rev. B 10, 3471 (1974).

[10]V. T. Nguyen, T. C. Damen, and E. Gornik, Appl. Phys. Lett. 30, 33 (1977).

[11]T. C. Damen, V. T. Nguyen, and E. Gornik, Solid State Commun. 24, 179 (1977).

[12]V. T. Nguyen, T. C. Damen, E. Gornik, and C. K. N. Patel, Appl. Phys. Lett. 31, 603 (1977).

[13]J. Jackel and H. Mahr, Phys. Rev. B 17, 3387 (1978).

[14]D. G. Seiler, D. Heiman, R. Feigenblatt, R. L. Aggarwal, and B. Lax, Phys. Rev. B 25, 7666 (1982).

[15]D. G. Seiler, M. W. Goodwin, and M. H. Weiler, Phys. Rev. B 23, 6806 (1981).

[16]M. W. Goodwin, D. G. Seiler, and M. H. Weiler, Phys. Rev. B 25, 6300 (1982).

[17]R. L. Byer, Electro-Opt. Syst. Des. 12, 24 (1980).

[18]G. D. Mahan and J. J. Hopfield, Phys. Rev. 135, A428 (1964).

[19]R. Dinges, D. Frohlich, B. Staginnus, and W. Staude, Phys. Rev. Lett. 25, 922 (1970).

[20]E. S. Koteles and G. Winterling, Phys. Rev. Lett. 44, 948 (1980).

[21]I. Broser and M. Rosenzweig, Phys. Status Solidi B 95, 141 (1979).

[22]B. Segall and D. T. F. Marple, in *Physics and Chemistry of II-VI Compounds,* edited by M. Aven and J. J. Prener (North-Holland, Amsterdam, 1967), Chap. 7, p. 344.